AIP | Physics of Fluids

Stokes number effects on particle slip velocity in wall-bounded turbulence and implications for dispersion models

L. H. Zhao, C. Marchioli, and H. I. Andersson

Citation: Phys. Fluids **24**, 021705 (2012); doi: 10.1063/1.3690071
View online: http://dx.doi.org/10.1063/1.3690071
View Table of Contents: http://pof.aip.org/resource/1/PHFLE6/v24/i2
Published by the American Institute of Physics.

Stokes number effects on particle slip velocity in wall-bounded turbulence and implications for dispersion models

L. H. Zhao,[1] C. Marchioli,[2] and H. I. Andersson[1]
[1]*Department of Energy and Process Engineering, Norwegian University of Science and Technology, 7491 Trondheim, Norway*
[2]*Department of Energy Technology, University of Udine, 33100 Udine, Italy*

(Received 30 September 2011; accepted 9 February 2012;
published online 29 February 2012)

The particle slip velocity is adopted as an indicator of the behavior of heavy particles in turbulent channel flow. The statistical moments of the slip velocity are evaluated considering particles with Stokes number, defined as the ratio between the particle response time and the viscous time scale of the flow, in the range $1 < St < 100$. The slip velocity fluctuations exhibit a monotonic increase with increasing particle inertia, whereas the fluid-particle velocity covariance is gradually reduced for $St \geq 5$. Even if this covariance equals the particle turbulence intensity, a substantial amount of particle slip may occur. Relevant to two-fluid modeling of particle-laden flows is the finding that the standard deviation of the slip velocity fluctuations is significantly larger than the corresponding mean slip velocity. © *2012 American Institute of Physics*. [http://dx.doi.org/10.1063/1.3690071]

The motion of a tiny solid particle in a turbulent flow is characterized by its Lagrangian velocity vector, $\mathbf{u}_p$. When the particle velocity differs from that of the surrounding fluid, e.g., due to particle inertia[1] or gravity,[2] significant decorrelation of the fluid velocity fluctuations along the particle trajectory occurs and a *particle slip velocity* can be observed. The particle slip velocity vector, defined as $\Delta\mathbf{u} = \mathbf{u}_f - \mathbf{u}_p$ with $\mathbf{u}_f$ the fluid velocity at the particle location (referred to as *fluid velocity seen* hereinafter), is a primary variable in two-fluid modeling of particle-laden flows,[3,4] for which new data might provide useful guidance. Its importance has long been recognized[5] with reference to crossing trajectory effects on the time decorrelation tensor of $\mathbf{u}_f$, a crucial parameter for the development of Lagrangian stochastic models of particle dispersion, for instance in gas-solid turbulent flows,[2] but also for the closure of Eulerian models.[6–8] More recently, accurate characterization of the slip velocity has become a key issue in modeling particle dynamics at the sub-grid scale level in large-eddy simulations.[9] The particle slip velocity is furthermore an outstanding measure of the interactions between the discrete particle phase and the continuous fluid phase being the only flow variable which determines (together with some fluid and particle physical properties) the drag experienced by the particles. The reaction force from the particles on the fluid in two-way coupled simulations is equally dependent on $\Delta\mathbf{u}$, which accordingly is essential for the modulation of the turbulent flow field.[10]

In this letter, we examine from a statistical viewpoint the slip velocity of particles with different inertia to explore their dynamics in turbulent channel flows and to provide information for possible inclusion in models. To these aims, statistics are computed considering conditional averaging rather than averaging on discrete Eulerian grid points. We used pseudo-spectral direct numerical simulation[9,11] of turbulent Poiseuille flow (incompressible and Newtonian) in a channel at $Re_\tau = u_\tau h/\nu = 150$, where $u_\tau = \sqrt{\tau_w/\rho}$ is the friction velocity with τ_w the wall shear stress and ρ the fluid density, ν is the kinematic fluid viscosity, and h is the channel half-height. The reference geometry consists of two infinite flat parallel walls with periodic boundary conditions in the streamwise (x) and spanwise (y) directions and no-slip conditions in the wall-normal direction (z).

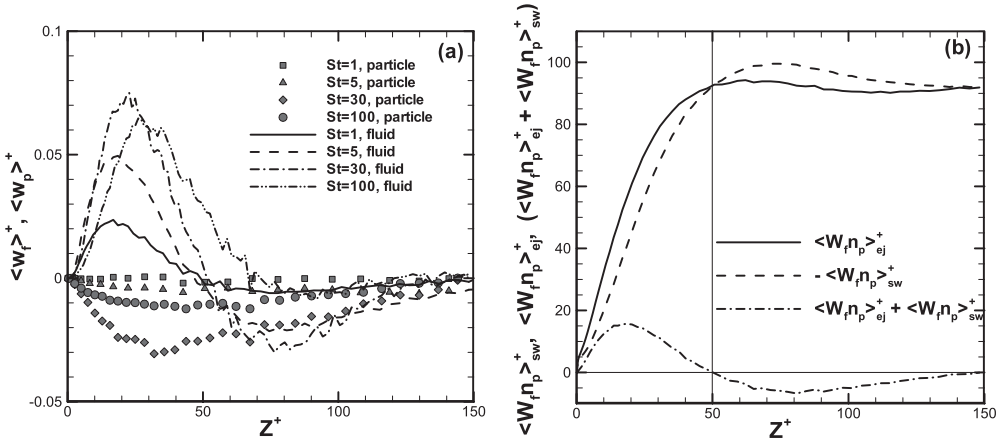

FIG. 1. (a) Mean values of the wall-normal component of the fluid velocity seen, $\langle w_f \rangle^+$, and of the particle velocity, $\langle w_p \rangle^+$. (b) Density-weighted fluid velocities seen by particles entrained in ejections or sweeps for $St = 5$.

The computational domain has dimensions (L_x, L_y, L_z)= ($4\pi h$, $2\pi h$, $2h$), discretized with 128^3 grid nodes.[12] We tracked swarms $-O(10^5)$ − of particles, treated as pointwise, rigid, elastically rebounding spheres with Stokes number $St = \tau_p/\tau_f = 1$, 5, 30, and 100. Here, $\tau_p = \rho_p d_p^2/18\mu$ is the particle characteristic time scale, with ρ_p and d_p the particle density and diameter, respectively, and $\tau_f = \nu/u_\tau^2$ is the viscous time scale of the flow. To characterize the collective behavior of particles, we chose a simplified numerical setting (one-way coupling approach) that applies to dilute flow regimes. Our findings are thus valid in the limit of negligible turbulence modulation and particle–particle interactions. One-way coupling also allows to investigate slip velocity statistics by letting different-inertia particles evolve in the same instantaneous flow field.

In many real applications the slip velocity is strongly influenced by gravity which acts to decorrelate the particle velocity from the fluid velocity seen.[2,5] In this work, gravity is ignored to isolate effects due solely to turbulence, and the Lagrangian equation of particle motion includes only inertia and Schiller-Naumann corrected Stokes drag[13] aimed to allow for finite particle Reynolds numbers. In vector form: $\mathrm{d}\mathbf{u}_p/\mathrm{d}t = (\Delta u/\tau_p)[1 + 0.15(|\Delta\mathbf{u}|d_p/\nu)^{0.687}]$. The results shown in this paper are given in wall units (obtained using ν and u_τ, and identified with superscript "+"), and were validated by running simulations with two independent codes.[9,11] Statistics were collected over a time window $\Delta t^+ = 3900$ starting at time $t^+ = 3000$ after particle injection: within this window slip velocity statistics are at steady state, while particle concentration and transport fluxes are not.[12] In Fig. 1(a), we contrast the wall-normal particle velocity ($\langle w_p \rangle^+$, symbols) against the wall-normal fluid velocity seen ($\langle w_f \rangle^+$, lines) at varying particle inertia. Brackets $\langle \ldots \rangle$ denote variables averaged in time and space (over the homogeneous directions x and y). Focusing first on particle velocity, it can be seen that the profiles exhibit the same qualitative behavior but differ quantitatively. All profiles start from zero in the channel center, attain negative values as the wall is approached (indicating that $\langle w_p \rangle^+$ is directed to the wall), develop a maximum in the region $20 < z^+ < 50$, and drop again to zero at the wall. This behavior was observed before for $St < 25$ (Ref. 14) and is a manifestation of a net particle flux toward the wall. From a quantitative viewpoint, inertia induces strong changes in the magnitude of $\langle w_p \rangle^+$: in the region where $\langle w_p \rangle^+$ develops a maximum, a decrease of more than one order of magnitude is observed for the $St = 1$ and $St = 5$ particles compared to the $St = 30$ particles. A decrease of $\langle w_p \rangle^+$ is found also for the $St = 100$ particles, confirming that wall accumulation increases with inertia up to an *optimum* value of the Stokes number ($St = 30$ in this study), while decreasing on either side of the optimum.

This non-monotonic Stokes number dependence is observed also for the fluid velocity seen. Another interesting feature, relevant for the present analysis, is that $\langle w_f \rangle^+$ undergoes a sign change while approaching the wall and becomes positive in the region where $\langle w_p \rangle^+$ reaches large negative values. A straightforward interpretation of this result would lead to conclude that particles move

toward the wall within regions of the flow where the fluid moves away from wall. This conclusion is however incorrect, as the phenomenology of near-wall turbulence is ignored. Regions characterized by off-the-wall fluid velocity represent coherent ejections of low momentum fluid away from the wall, which co-exist with coherent sweeps of high-momentum fluid to the wall. Sweeps and ejections are known to govern particle transfer flux to/off the wall,[1] and it is precisely their capability to entrain particles and modulate the flow field seen that generates the counter-intuitive behavior of $\langle w_f \rangle^+$. This is demonstrated, only for the $St = 5$ particles to simplify discussion, in Fig. 1(b) where we plot the density-weighted fluid velocity seen by particles entrained either in ejections, $\langle w_f \cdot n_p \rangle^+_{ej}$ with $w_f > 0$, or in sweeps, $\langle w_f \cdot n_p \rangle^+_{sw}$ with $w_f < 0$. The quantity n_p denotes particle number density. We also plot the sum $\langle w_f \cdot n_p \rangle^+_{ej} + \langle w_f \cdot n_p \rangle^+_{sw}$, which is almost proportional to the dashed $\langle w_f \rangle^+$ profile shown in Fig. 1(a). Near the wall ($z^+ < 50$ in our simulations), $\langle w_f \cdot n_p \rangle^+_{ej} > \langle w_f \cdot n_p \rangle^+_{sw}$ and therefore $\langle w_f \rangle^+ > 0$ even if $\langle w_p \rangle^+ < 0$. The opposite reasoning applies away from the wall. From a physical viewpoint, this behavior can be explained interpreting particle preferential sampling of $\langle w_f \rangle^+ > 0$ regions as a sort of continuity effect of the fluid velocity field for which sweeps are more intense and spatially concentrated than ejections.[14] In addition, sweeps dominate Reynolds stress production very near the wall whereas ejections dominate farther from it:[1] hence, the ejection-dominated region covers a much wider proportion of the $z^+ < 50$ fluid slab.

The deviations between $\langle w_p \rangle^+$ and $\langle w_f \rangle^+$ observed in Fig. 1 indicate that the slip velocity is largely dependent on the wall distance, z^+. Let us now decompose the slip velocity vector into a mean and a fluctuating part:

$$\langle \Delta \mathbf{u} \rangle = \langle \mathbf{u}_f \rangle - \langle \mathbf{u}_p \rangle, \quad \Delta \mathbf{u}' = \mathbf{u}'_f - \mathbf{u}'_p. \tag{1}$$

The streamwise and wall-normal mean slip velocity components, $\langle \Delta u \rangle^+$ and $\langle \Delta w \rangle^+$, are shown in Figs. 2(a) and 2(b) together with the corresponding standard deviations (root-mean-square values), $\mathrm{rms}(\Delta u')^+$ and $\mathrm{rms}(\Delta w')^+$, shown in Figs. 2(c) and 2(d). First, we notice that the streamwise mean slip velocity $\langle \Delta u \rangle^+$ shows the same characteristic variation regardless of the Stokes number: negative values near the wall ($z^+ < 20$), indicating that the particles lead the fluid, positive values throughout the central region, where the particles lag behind the fluid. This behavior is known from mean velocity profiles.[14] The sign change of $\langle \Delta u \rangle^+$ implies that the direction of the mean drag force changes with the distance from the wall. Interestingly, this change occurs at $z^+ \simeq 18$ irrespective of the Stokes number. Second, we observe that the magnitude of the mean slip velocities increases monotonically with St: in the core region of the channel, this increase indicates that the ability of particles to adapt to the fluid motion is gradually reduced with increasing inertia; closer to the wall, it corresponds to an increased capability of maintaining streamwise momentum while drifting to the wall due to turbophoresis. This explains why $\langle u_p \rangle$ exceeds $\langle u_f \rangle$ near the wall. Arcen *et al.*[15] found a similar variation of the streamwise drag force per unit mass, but also observed a drag decrease with increasing particle inertia in the range $1.2 < St < 27.1$. This reduction stems from the increasing St since the drag force to a first approximation is proportional to $\Delta u/St$.

The wall-normal component of the mean slip velocity, shown in Fig. 2(b), is largest for the $St = 30$ particles as follows from discussion of Fig. 1, and attains positive values for $z^+ < 50$ regardless of the Stokes number. This implies that the mean drag force counteracts particle drift to the wall within the buffer layer. In the core region, particles with low inertia are driven to the wall by a negative mean drag force, whereas large-inertia particles ($St \geq 30$) still experience a weak positive drag force. Figures 2(c) and 2(d) show that the streamwise and wall-normal slip velocity fluctuations increase monotonically with St. Profiles of $\mathrm{rms}(\Delta v')^+$ (not shown) exhibit the same trend, suggesting that the slip velocity fluctuations are weakly influenced by the inertial bias that shows in the behavior of $\langle \Delta w \rangle^+$. It is noteworthy that the largest values of $\mathrm{rms}(\Delta u')^+$ occur close to the wall, with peaks located in the buffer layer for both the heavier $St = 100$ particles ($z^+ \simeq 11$) and the lighter $St = 1$ particles ($z^+ \simeq 9$). The opposite behavior is observed for $\mathrm{rms}(\Delta w')^+$, whose maximum values shift away from the wall at increasing particle inertia: the peak is located well outside the buffer layer (at $z^+ \simeq 45$) for $St = 100$. The most relevant result provided by Fig. 2, however, is the magnitude of the rms values over the channel cross section. Regardless of the coordinate direction, the standard

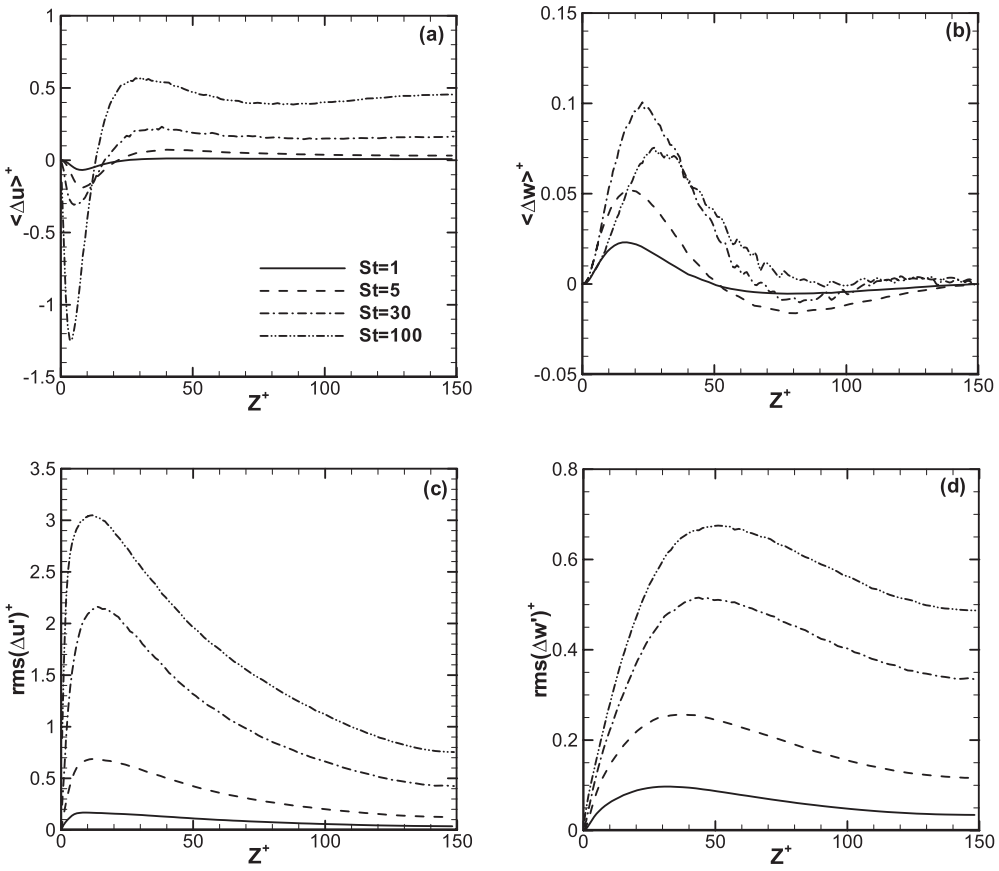

FIG. 2. Stokes number effects on mean and rms slip velocity statistics: (a–b) mean streamwise and wall-normal slip velocity, $\langle \Delta u \rangle^+$ and $\langle \Delta w \rangle^+$; (c–d) rms of streamwise and wall-normal slip velocity fluctuations, $\langle \mathrm{rms}(\Delta u') \rangle^+$ and $\langle \mathrm{rms}(\Delta w') \rangle^+$.

deviation typically exceeds the corresponding mean value by roughly 3 to 5 times, revealing that the instantaneous slip velocity and, in turn, the drag force may frequently change sign.

A more complete understanding of the statistical characterization of $\mathrm{rms}(\Delta \mathbf{u}')$ can be achieved if the fluctuating slip velocity components are normalized either by the fluid velocity fluctuations along the particle trajectories, as in Figs. 3(a) and 3(b), or by the particle velocity fluctuations, as in Figs. 3(c) and 3(d). All profiles in Fig. 3 increase monotonically with the Stokes number. Profiles in Figs. 3(a) and 3(b) are nearly flat outside of the buffer layer, i.e., beyond $z^+ \approx 30$. In this region, the rms ratio is rather low for the $St = 1$ particles since these light particles closely follow the local fluid motion and therefore exhibit small standard deviations compared to the fluid; the heavier $St = 100$ particles tend to move independently of the fluid and one may conjecture that $\mathrm{rms}(\Delta \mathbf{u}') \approx \mathrm{rms}(\mathbf{u}'_f)$ in the limit $St \to \infty$. Inside the viscous sub-layer, however, the rms ratios attain values significantly above unity. The fluid velocity fluctuations are substantially damped in the immediate vicinity of the solid wall, whereas the inertial particles are able to maintain the momentum acquired farther from it during their interaction with the turbulent coherent structures. This behavior has been observed also in a spatially developing turbulent boundary layer[16] where the globally averaged rms ratios may exceed unity and, consistently with our findings, increase with St. Rms ratios close to unity are observed at the wall in Figs. 3(c) and 3(d) except for the lighter particles. Thus, for particles with $St \geq 30$ the slip velocity fluctuations $\mathrm{rms}(\Delta \mathbf{u}')$ in the vicinity of the wall stem from the particle velocity fluctuations $\mathrm{rms}(\mathbf{u}'_p)$ since the fluid velocity fluctuations $\mathrm{rms}(\mathbf{u}'_f)$ are suppressed by the no-slip and

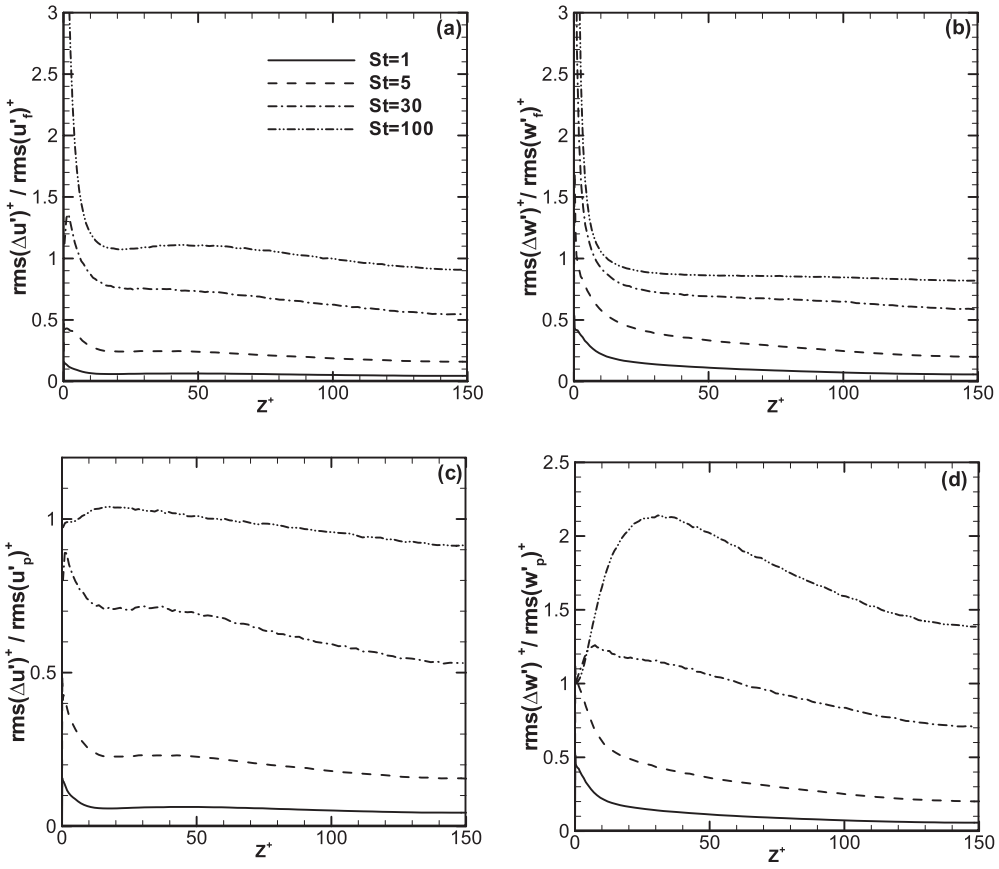

FIG. 3. Stokes number effects on the rms of slip velocity fluctuations normalized either by the rms of the fluid velocity fluctuations along the particle trajectory (a–b) or by the rms of the particle velocity fluctuations (c–d).

impermeability conditions imposed at the wall. The variation of the rms ratios in the core region of the channel resembles the trends observed in Figs. 3(a) and 3(b).

We conclude our discussion by considering the fluid-particle velocity *covariance*, an important quantity in Lagrangian[3] and Eulerian models,[6,8] e.g., to compute integral time scales. For the present analysis, the streamwise and wall-normal components, $\langle u'_f u'_p \rangle$ and $\langle w'_f w'_p \rangle$, respectively, are the

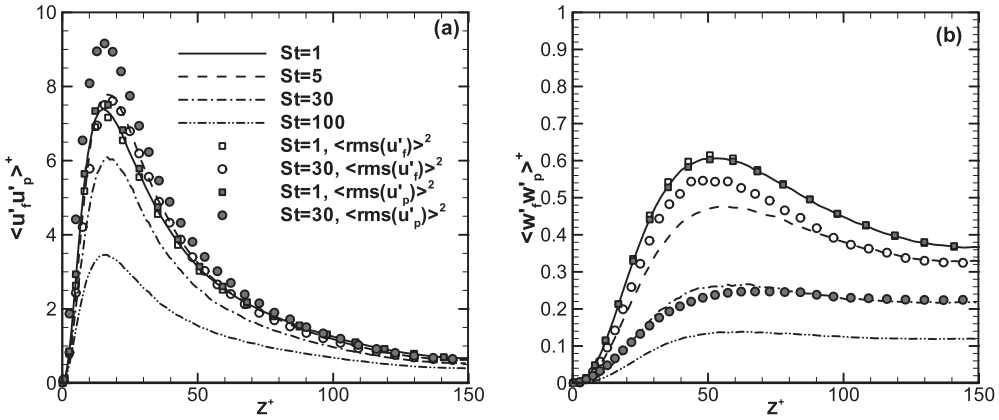

FIG. 4. Stokes number effects on the fluid-particle velocity covariance. Panels: (a) streamwise covariance, $\langle u'_f u'_p \rangle$; (b) wall-normal covariance, $\langle w'_f w'_p \rangle$. Fluid and particle fluctuations ($St = 1$ and 30 only) are also shown for comparison purposes (open symbols: $\langle \mathrm{rms}(u'_f) \rangle^2$; filled symbols: $\langle \mathrm{rms}(u'_p) \rangle^2$).

most interesting. In agreement with previous observations,[15,17] Fig. 4 shows that $\langle u'_f u'_p \rangle$ exceeds $\langle w'_f w'_p \rangle$ and that both components are substantially reduced as St increases. The only exception from this general trend is the modest, yet significant increase of $\langle u'_f u'_p \rangle$ for the $St = 5$ particles as compared with the $St = 1$ particles. This increase was not observed by Arcen *et al.*,[15,18] who however adopted slightly different values of Re_τ and St and no drag force correction, nor by Vance *et al.*,[17] who focused on relatively heavy particles ($30 \leq St \leq 470$).

The streamwise covariance is related to the streamwise slip velocity fluctuations through the equality:

$$\langle \Delta u'^2 \rangle = \langle u'^2_f \rangle - 2\langle u'_f u'_p \rangle + \langle u'^2_p \rangle. \tag{2}$$

Analogous equalities apply in the other coordinate directions. Since both fluid and particle intensities in the streamwise direction are modestly affected by the particle Stokes number, the reduction of $\langle u'_f u'_p \rangle$ observed in Fig. 4(a) is directly linked to the increase of $\langle \Delta u'^2 \rangle$ in Fig. 2(c). For the lower Stokes numbers, $\langle u'_f u'_p \rangle \approx \langle u'^2_p \rangle$ and one can therefore infer from Eq. (2) that: $\langle \Delta u'^2 \rangle = \langle u'^2_f \rangle - \langle u'^2_p \rangle$. However, it can by no means be concluded that the slip velocity fluctuations vanish and that the particles exactly follow the local fluid motion, i.e., that $\langle u'^2_p \rangle \approx \langle u'^2_f \rangle$. For $St = 1$, Fig. 4(a) shows that the results are fairly close to this limit and Fig. 4(b) shows that $\langle w'_f w'_p \rangle \approx \langle w'^2_p \rangle \approx \langle w'^2_f \rangle$, which is consistent with the almost negligible slip fluctuations $\langle \Delta w'^2 \rangle$ in Fig. 2(d). For the heavier $St = 30$ particles $\langle w'_f w'_p \rangle \approx \langle w'^2_p \rangle \ll \langle w'^2_f \rangle$, hence the condition $\langle w'_f w'_p \rangle \approx \langle w'^2_p \rangle$ which applies to low- or intermediate-St particles is not sufficient to warrant that particles passively follow the fluid, as argued by Vance *et al.*[17] This conclusion is in accordance with the Cauchy-Schwartz inequality: $\langle w'_f w'_p \rangle^2 \leq \langle w'^2_f \rangle \langle w'^2_p \rangle$ from which one can only deduce that $\langle w'_f w'_p \rangle^2 \leq \langle w'^2_f \rangle^2$ in such cases, e.g., that of Fig. 4(b). In the limit of $St \to \infty$, particle motion is not at all influenced by the flow field and u'_p is completely suppressed. Equation (2) accordingly simplifies to $\langle \Delta u'^2 \rangle = \langle u'^2_f \rangle$. Inspections of the data presented in Figs. 3 and 4 demonstrate that even the results for the heaviest $St = 100$ particles are far apart from this limit, although these particles experience a substantial velocity slip.

In this letter we have demonstrated that the particle slip velocity is a useful measure of particle-turbulence interactions in wall-bounded flows and that its statistical characterization may provide new information about the physics and useful indications for modeling turbulent particle dispersion. To summarize, our results show that the slip velocity fluctuations $\Delta \mathbf{u}'$ are significantly larger than the corresponding mean slip velocity $\langle \Delta \mathbf{u} \rangle$, with the consequence that a given directional component of the instantaneous slip velocity vector $\Delta \mathbf{u}$ may frequently attain the sign opposite to that of $\langle \Delta \mathbf{u} \rangle$. The statistical behavior of the slip velocity is thus expected to depend strongly on the distribution of the turbulent velocity fluctuations, which is highly anisotropic in wall-bounded flows. We have also pointed out that the condition of particle-fluid covariance equals to the particle turbulence intensity in a given direction is not sufficient to ensure that particles passively follow the fluid motion.

Computing time was granted by CINECA Supercomputing Center (Bologna, Italy), which also provided data storage (http://cfd.cineca.it), and by the Research Council of Norway (Programme for Supercomputing). COST Actions MP0806 and FP1005 are gratefully acknowledged. C.M. also thanks Professor A. Soldati for providing part of the raw data that were used in this study.

[1] C. Marchioli and A. Soldati, "Mechanisms for particle transfer and segregation in turbulent boundary layer," J. Fluid Mech. **468**, 283 (2002).
[2] B. Oesterlé, "On heavy particle dispersion in turbulent shear flows: 3-D analysis of the effects of crossing trajectories," Boundary-Layer Meteorol. **130**, 71 (2009).
[3] B. Arcen and A. Tanière, "Simulation of a particle-laden turbulent channel flow using an improved stochastic Lagrangian model," Phys. Fluids **21**, 043303 (2009).
[4] X. Pialat, O. Simonin, and P. Villedieu, "A hybrid Eulerian-Lagrangian method to simulate the dispersed phase in turbulent gas-particle flows," Int. J. Multiphase Flow **33**, 766 (2007).
[5] G. T. Csanady, "Turbulent diffusion of heavy particles in the atmosphere," J. Atmos. Sci. **20**, 201 (1963).
[6] O. Simonin, E. Deutsch, and J. P. Minier, "Eulerian prediction of fluid-particle correlated motion in turbulent two-phase flows," Appl. Sci. Res. **51**, 275 (1993).
[7] S. Cerbelli, A. Giusti, and A. Soldati, "ADE approach to predicting dispersion of heavy particles in wall-bounded turbulence," Int. J. Multiphase Flow **27**, 1861 (2001).

[8] M. W. Reeks, "On model equations for particle dispersion in inhomogeneous turbulence," Int. J. Multiphase Flow **31**, 93 (2005).
[9] A. Soldati and C. Marchioli, "Physics and modelling of turbulent particle deposition and entrainment: Review of a systematic study," Int. J. Multiphase Flow **35**, 827 (2009).
[10] L. H. Zhao, H. I. Andersson, and J. J. J. Gillissen, "Turbulence modulation and drag reduction by spherical particles," Phys. Fluids **22**, 081702 (2010).
[11] J. J. J. Gillissen, B. J. Boersma, P. H. Mortensen, and H. I. Andersson, "On the performance of the moment approximation for the numerical computation of fibre stress in turbulent channel flow," Phys. Fluids **19**, 035102 (2007).
[12] C. Marchioli, A. Soldati, J. G. M. Kuerten, B. Arcen, A. Tanière, G. Goldensoph, K. D. Squires, M. F. Cargnelutti, and L. M. Portela, "Statistics of particle dispersion in direct numerical simulations of wall-bounded turbulence: Results of an international collaborative benchmark test," Int. J. Multiphase Flow **34**, 879 (2008).
[13] L. Schiller and A. Z. Naumann, "Über die grundlegenden Berechnungen bei der Schwerkraftaufbereitung," Z. Ver. Dtsch. Ing. **77**, 318 (1933).
[14] M. Picciotto, C. Marchioli, M. Reeks, and A. Soldati, "Statistics of velocity and preferential accumulation of micro-particles in boundary layer turbulence," Nucl. Eng. Des. **235**, 1239 (2005).
[15] B. Arcen, A. Tanière, and B. Oesterlé, "On the influence of near-wall forces in particle-laden channel flows," Int. J. Multiphase Flow **32**, 1326 (2006).
[16] A. Dorgan and E. Loth, "Simulation of particles released near the wall in a turbulent boundary layer," Int. J. Multiphase Flow **30**, 649 (2004).
[17] M. W. Vance, K. D. Squires, and O. Simonin, "Properties of the particle velocity field in gas-solid turbulent channel flow," Phys. Fluids **18**, 063302 (2006).
[18] B. Arcen, A. Tanière, and L. I. Zaichik, "Assessment of a statistical model for the transport of discrete particles in a turbulent channel flow," Int. J. Multiphase Flow **34**, 419 (2008).